Quantum Electronics **35** (1) 69 – 79 (2005)

QUANTUM OPTICS AND QUANTUM COMPUTATION

PACS numbers: 42.50.Dv; 42.65.Lm
DOI: 10.1070/QE2005v035n01ABEH002891

Polarisation properties of single-mode biphotons

L.A. Krivitsky, S.P. Kulik, G.A. Maslennikov, M.V. Chekhova

***Abstract*. The paper reviews recent research by the authors on the polarisation properties of correlated photon pairs, also called biphotons, generated via spontaneous parametric down-conversion in the collinear frequency – degenerate regime. From the viewpoint of their polarisation properties, they represent qutrits, i.e., three-dimensional quantum systems, and are quite promising for quantum information applications.**

Keywords: *biphotons, polarisation properties, spontaneous parametric down-conversion.*

1. Introduction

Biphoton light, i.e., light consisting of correlated photon pairs (biphotons), is one of the few types of nonclassical light now reliably generated in laboratories. Biphoton light has some unique properties, which, as a rule, cannot be explained within the framework of classical optics and are employed in quantum optics, quantum information, and quantum metrology. Due to the applications of entangled two-photon states in quantum information [1, 2], the polarisation properties of biphoton light become more and more significant. However, most works studying the polarisation properties of biphotons relate to the case of two spatial or frequency modes, for which a comprehensive description in terms of Bell states has been developed [3, 4]. Bell states of the biphoton field have been used for the 'dense coding' of quantum information [5], in quantum metrology (for the absolute calibration of photodetectors) [6], in experiments on 'entanglement swapping' [7], in quantum teleportation experiments [8], and in quantum cryptography [9]. Characterisation ('tomography') methods for these states have been developed [10].

At the same time, little attention has been paid to the study of the polarisation states of biphotons belonging to a single spatial and frequency mode (hereafter called single-mode biphotons, although this term is not quite correct because two polarisation modes are always considered). The polarisation description of such states was first suggested by Klyshko in Ref. [11] and further developed in Ref. [12]. The analysis showed that the symmetry and transformation properties of these states are similar to the properties of quarks. According to this, such states can be called qutrits [13], by analogy with qubits [14], quantum information bits. The present review includes a series of works by the authors carried out in 1998 – 2004 and devoted to a more detailed investigation of such states, their preparation in experiment by means of spontaneous parametric down-conversion (SPDC), transformations by means of linear polarisation elements, and further measurement.

L.A. Krivitsky, S.P. Kulik, G.A. Maslennikov, M.V. Chekhova
Department of Physics, M.V. Lomonosov Moscow State University, Vorob'evy gory, 119992 Moscow, Russia;
e-mail: masha@qopt.phys.msu.su

Received 30 September 2004; revision received 26 November 2004
Kvantovaya Elektronika **35** (1) 69 – 79 (2005)
Translated by M.V. Chekhova

2. Polarisation state of a biphoton and its different representations

Consider the state of two-photon light generated via collinear frequency-degenerate SPDC. For simplicity, we analyse an ideal case where the field contains only a single space and frequency mode. An arbitrary polarisation state of such a field has the form [12]

$$|\Psi\rangle = c_1|2,0\rangle + c_2|1,1\rangle + c_3|0,2\rangle, \quad (1)$$

where $|n,m\rangle$ denotes the state with m photons in the H polarisation mode and n photons in the orthogonal polarisation mode V. In addition, the vacuum component $|\mathrm{vac}\rangle$ is omitted in Eqn (1), because it is not significant for the effects under study. The first and the third terms in (1) can be obtained in experiment via SPDC with type-I phase matching while the second one, via SPDC with type-II phase matching. Because of the normalisation, $|c_1|^2 + |c_2|^2 + |c_3|^2 = 1$, and the insignificance of the total phase of the wavefunction, the state (1) can be characterised by four real parameters d_1, d_3, φ_2, φ_3 ($c_i \equiv d_i \exp(\mathrm{i}\varphi_i)$, $\sum d_i^2 = 1$ ($i = 1, 2, 3$), $\varphi_1 = 0$, φ_2, $\varphi_3 \in [0, 2\pi]$) [12]. Note that hereafter (except the cases that will be specially discussed), the biphoton state is assumed to be pure; a mixed state of a biphoton should be characterised by a larger set of parameters. Similarly to the way a classical polarisation state of light can be denoted by a point on the Poincare sphere (a sphere S^2 in the space R^3) [15], the state of two-photon light (1) can be denoted by a point on a four-dimensional sphere (S^4) in a five-dimensional space (R^5). Accordingly, the vector $\boldsymbol{e} = (c_1, c_2, c_3)$ can be called the polarisation vector of a biphoton [12].

In Ref. [16], a more explicit way was proposed to geometrically interpret the polarisation state of a biphoton. One can show that the state vector (1) can be equivalently represented as

$$|\Psi\rangle = \frac{a^+(\vartheta,\varphi)a^+(\vartheta',\varphi')|\mathrm{vac}\rangle}{||a^+(\vartheta,\varphi)a^+(\vartheta',\varphi')|\mathrm{vac}\rangle||}. \quad (2)$$

Here, $a^+(\vartheta,\varphi)$ and $a^+(\vartheta',\varphi')$ are photon creation operators in arbitrary polarisation modes: $a^+(\vartheta,\varphi) = a_{\mathrm{H}}^+ \times \cos(\vartheta/2) + a_{\mathrm{V}}^+ \exp(\mathrm{i}\varphi)\sin(\vartheta/2)$; $a_{\mathrm{H,V}}^+$ are photon creation operators in linear polarisation modes H, V; $\varphi, \varphi' \in [0, 2\pi]$ and $\vartheta, \vartheta' \in [0, \pi]$ are, respectively, the azimuth and polar angles on the Poincare sphere. Without the normalisation, the norm of the state vector (2) would vary from unity [in the case where $a^+(\vartheta,\varphi)$ and $a^+(\vartheta',\varphi')$ are orthogonal] to two [in the case where $a^+(\vartheta,\varphi)$ and $a^+(\vartheta',\varphi')$ coincide]. In terms of the spherical coordinates ϑ, ϑ', φ, φ', the squared norm can be expressed as

$$|\Psi|^2 = 1 + \cos^2\frac{\vartheta-\vartheta'}{2} - \sin\vartheta\sin\vartheta'\sin^2\frac{\varphi-\varphi'}{2}. \quad (3)$$

Transformations from the angles $\{\vartheta, \vartheta', \varphi, \varphi'\}$ to the amplitudes and phases $\{d_1, d_3, \varphi_2, \varphi_3\}$ as well as the inverse transformations are rather bulky and are given in Ref. [16].

Thus, an arbitrary state of a degenerate biphoton field can be shown by two points on the Poincare sphere and given by four parameters, ϑ, ϑ', φ, φ'. For instance, the state $|2,0\rangle$ is depicted by a 'double point' on the sphere and the state $|1,1\rangle$, by two points on the opposite sides of a single diameter (Fig. 1). The Stokes vector for biphoton light is given by the sum of the Stokes vectors $\boldsymbol{S}$ and $\boldsymbol{S}'$ for the states $a^+(\vartheta,\varphi)|\mathrm{vac}\rangle$ and $a^+(\vartheta',\varphi')|\mathrm{vac}\rangle$ divided by $|\Psi|^2$, and the polarisation degree P is determined by the cosine of the angle σ between the vectors $\boldsymbol{S}$ and $\boldsymbol{S}'$:

$$P = \frac{2\cos(\sigma/2)}{1+\cos^2(\sigma/2)}. \quad (4)$$

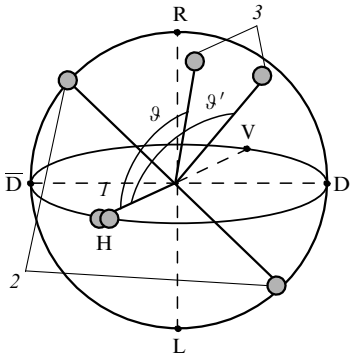

Figure 1. Representation of the state (2) of an arbitrary polarised biphoton on the Poincare sphere as two correlated arbitrarily polarised photons: (*1*) state $|2,0\rangle$, i.e., a pair of correlated photons polarised linearly along the H axis; (*2*) state of two correlated orthogonally polarised photons; (*3*) state of a biphoton in an arbitrary polarisation state.

Note that (4) is the usual ('single-photon') polarisation degree, which is defined in terms of the Stokes parameters. There also exist special definitions for the 'two-photon' polarisation degree [17–19] but we will not consider them here since they can be shown to be related to the purity of the state. In particular, for a pure state of the form (1), two-photon polarisation degree is always equal to unity. Let us give some examples of biphoton states.

1. For $d_2 = 0$, we obtain

$$\cos\frac{\vartheta}{2} = \left(\frac{d_1}{d_1+d_3}\right)^{1/2}, \quad \varphi = \varphi_3, \quad \vartheta' = \vartheta, \quad \varphi' = \pi + \varphi.$$

Such states can be shown in Fig. 1 by pairs of points symmetric with respect to the HV axis.

2. For $d_1 = d_2 = d_3 = 1/\sqrt{3}$, $\varphi_2 = \varphi_3 = 0$ the state can be shown in Fig. 1 by a pair of points in the plane $\mathrm{D}\overline{\mathrm{D}}$, RL at angles $\pm 45^\circ$ to the $\mathrm{D}\overline{\mathrm{D}}$ ($|\mathrm{D}\rangle \equiv |+45^\circ\rangle$, $|\overline{\mathrm{D}}\rangle \equiv |-45^\circ\rangle$) axis. The polarisation degree is $P = 2\sqrt{2}/3$.

3. For $d_1 = d_2 = d_3 = 1/\sqrt{3}$, $\varphi_2 = \pi/2$, $\varphi_3 = 0$, we obtain a non-polarized state (the polarisation degree is zero), which can be shown in Fig. 1 by a pair of points in the plane HV, RL on the opposite ends of a single diameter, so that $\vartheta = \arccos[1/(2\sqrt{3})]$, $\vartheta' = \pi - \arccos[1/(2\sqrt{3})]$.

Experimental preparation of an arbitrary biphoton polarisation state is very important for the transmission of quantum information. The corresponding experiments will be considered in Section 7.

3. Polarisation 'tomography' of single-mode biphotons

Polarisation state of a biphoton field (1) cannot be fully described by means of only standard polarisation measurements, such as, for instance, measurement of the Stokes parameters. The state (1) is most interesting from the standpoint of the fourth-order field moments. It was shown in Ref. [11] that the complete information about the fourth moment of polarised biphoton light is contained in the so-called fourth-order coherence matrix,

$$K_4 = \begin{pmatrix} A & D & E \\ D^* & C & F \\ E^* & F^* & B \end{pmatrix},$$

whose elements are normally-ordered moments of the fourth order in the field:

$$A \equiv \langle a_{\mathrm{H}}^{+2} a_{\mathrm{V}}^2\rangle, \quad B \equiv \langle a_{\mathrm{V}}^{+2} a_{\mathrm{V}}^2\rangle, \quad C \equiv \langle a_{\mathrm{H}}^{+} a_{\mathrm{V}}^{+} a_{\mathrm{H}} a_{\mathrm{V}}\rangle,$$
$$D \equiv \langle a_{\mathrm{H}}^{+2} a_{\mathrm{H}} a_{\mathrm{V}}\rangle, \quad E \equiv \langle a_{\mathrm{H}}^{+2} a_{\mathrm{V}}^2\rangle, \quad F \equiv \langle a_{\mathrm{H}}^{+} a_{\mathrm{V}}^{+} a_{\mathrm{V}}^2\rangle. \quad (5)$$

Here, A, B, C are real and D, E, F are complex numbers. In the general case of a biphoton mixed state, it is necessary to know all nine real numbers forming the matrix (if one knows the total photon number or the total energy, eight numbers are sufficient). However, for the characterisation of a pure state (1), it is sufficient to know only three real elements A, B, C and any two of the three complex elements D, E, F [11]. For instance, knowing A, B, C, D, and F, one can express the parameters of the state (1) as

$$d_1^2 = \frac{A}{A+B+2C}, \quad d_3^2 = \frac{B}{A+B+2C},$$
$$d_1 d_2 \exp(\mathrm{i}\varphi_2) = \frac{\sqrt{2}D}{A+B+2C}, \quad (6)$$
$$d_3 d_2 \exp[\mathrm{i}(\varphi_3 - \varphi_2)] = \frac{\sqrt{2}F}{A+B+2C}.$$

The case of a mixed state of the biphoton field can be interpreted as the existence of classical fluctuations for the amplitudes c_i in (1). Such a state should be described in terms of a density matrix whose nine elements are in one-to-one correspondence with the elements of the K_4 matrix.

James et al. [10] suggested a set of 16 measurements for the characterisation of a two-mode biphoton field*. Note that the matrix whose elements were measured in Ref. [10] in the single-mode case coincides with the K_4 matrix from [11]. Following the approach of Ref. [10], one can suggest a scheme for measuring the polarisation state of single-mode two-photon light [16] (Fig. 2). In this scheme, the biphoton beam is first split in two by means of a nonpolarising beamsplitter, and then measurements similar to the ones used in Ref. [10] are performed in each of the two beams. Into each beam, a combination of optical elements is inserted: a half-wave plate, a quarter-wave plate, and a linear polarisation filter oriented vertically. Then, one measures the coincidence counting rate for two detectors placed after the polarisation filters, for a certain set of phase plates positions. Due to the symmetry of the two beams (since the biphotons belong to a single mode), for a pure state it is sufficient to perform seven measurements instead of sixteen suggested in Ref. [10]**.

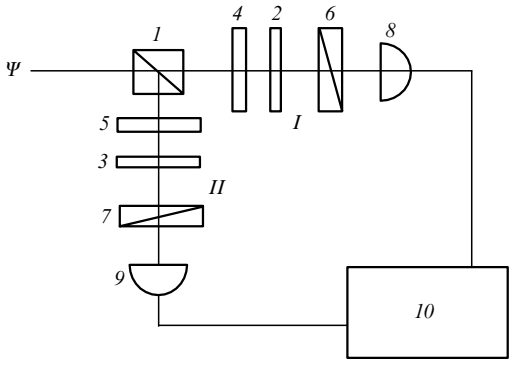

Figure 2. A setup for the polarisation tomography of single-mode biphoton light: (*1*) non-polarising beamsplitter; (*2*), (*3*) half-wave plates; (*4*), (*5*) quarter-wave plates; (*6*), (*7*) polarisation filters transmitting linearly polarised light; (8), (*9*) photodetectors; (*10*) coincidence circuit; (*I*), (*II*) interferometer arms.

Let us show how the elements of the K_4 matrix can be expressed in terms of the coincidence counting rate measured in the scheme of Fig. 2.

The coincidence counting rate is given by the correlator $G \equiv \langle a^{+\prime}_{\mathrm{V1}} a^{+\prime}_{\mathrm{V2}} a'_{\mathrm{V1}} a'_{\mathrm{V2}} \rangle$, where $a^{+\prime}_{\mathrm{V1}}$, $a^{+\prime}_{\mathrm{V2}}$ are photon creation operators for the vertical polarisation in modes 1, 2 after polarisation transformations. Photon creation operators after polarisation transformations can be expressed in terms of the photon creation operators before polarisation transformations a^{+}_{V1}, a^{+}_{V2} as

$$\begin{pmatrix} a^{+\prime}_{\mathrm{H1,H2}} \\ a^{+\prime}_{\mathrm{V1,V2}} \end{pmatrix} = D_{\mathrm{h}} D_{\mathrm{q}} \begin{pmatrix} a^{+}_{\mathrm{H1,H2}} \\ a^{+}_{\mathrm{V1,V2}} \end{pmatrix}. \tag{7}$$

Here, D_{h} and D_{q} are the Jones matrices for the quarter-wave and half-wave plates [11]. These matrices have the form

$$D = \begin{pmatrix} t & r \\ -r^* & t^* \end{pmatrix},$$

where t and r are, respectively, transmission and reflection complex coefficients. They can be written as

$$t = \cos\delta + \mathrm{i}\sin\delta\cos 2\chi, \quad r = \mathrm{i}\sin\delta\cos 2\chi, \tag{8}$$

where χ is the angle between the optic axis of a plate and the H axis and δ is the phase shift in the plate between the two waves of orthogonal polarisations (for instance, for a half-wave plate, $\delta = \pi/2$). Photon creation operators after the beamsplitter can be expressed via the corresponding operators before the beamplitter as

$$a^{+}_{\mathrm{H1,V1}} = \frac{a^{+}_{\mathrm{H,V}} + a^{+}_{\mathrm{H0,V0}}}{\sqrt{2}}, \quad a^{+}_{\mathrm{H2,V2}} = \frac{a^{+}_{\mathrm{H,V}} - a^{+}_{\mathrm{H0,V0}}}{\sqrt{2}}.$$

Here, the subscript 0 denotes the second input mode of the beamsplitter, which in the case under study is in the vacuum state. For this reason, the corresponding creation and annihilation operators will not enter the final result. A complete set of measurements is presented in Table 1, where orientations of the plates and the measured quantities are given.

Note that the set presented in Table 1 is not unique. It was chosen according to the requirement that the measured correlation function should contain the minimal possible number of elements of the coherence matrix. One can see that a complete set of measurements can be realised with a single quarter-wave plate and two half-wave plates or, if the polarisers can be rotated, with a single quarter-wave plate inserted in one beam. Thus, all measurements required for the characterisation of the biphoton field consist of the registration of coincidence counting rate between the two detectors. This measurement is repeated for various orientations of the optical elements preceding the detectors. Phase plates and linear polarisation analysers in each channel after the beamsplitter form filters for the selection of given polarisation states. For instance, in the measurement described by the first line of Table 1, these filters select linear vertical polarisation in both channels, while in the measurement described by the fifth line, left circular polarisation is selected in one channel and linear vertical polarisation is selected in another channel. In other words, in each channel the unknown input polarisation state is projected onto some fixed state. The method resembles the traditional tomography procedure where one and the same object is imaged from different space points, i.e., different sections of the same object are formed. It is namely this property that justifies the using of the term 'tomography' in this case, although the term is already accepted in quantum optics in relation to other measurements, like the Wigner function tomography [20–22] or tomography of the Stokes parameter fluctuations [23].

Note that although a pure polarisation state of a biphoton is characterised by only four parameters, its tomography includes a set of seven measurements. This is because, first, the total number of emitted biphotons, $(A + B + 2C)/2$, is unknown and should be measured and

* One can pass from the single-mode case to the two-mode one by assuming that the signal and idler photons have either different frequencies or different scattering angles.

** For a mixed single-mode state, nine measurements would be necessary.

Table 1. Set of measurements for the polarisation tomography of single-mode biphoton light.

Measurement number	Orientation angle/deg				Measured quantity
	quarter-wave plate (*4*)	half-wave plate (*2*)	quarter-wave plate (*5*)	half-wave plate (*3*)	
1	0	0	0	0	$\frac{1}{4}B$
2	0	45	0	45	$\frac{1}{4}A$
3	0	45	0	0	$\frac{1}{4}C$
4	45	22.5	0	0	$\frac{1}{8}(B+C-2\mathrm{Re}F)$
5	45	0	0	0	$\frac{1}{8}(B+C+2\mathrm{Im}F)$
6	0	45	45	22.5	$\frac{1}{8}(A+C-2\mathrm{Re}D)$
7	45	0	0	45	$\frac{1}{8}(A+C+2\mathrm{Im}D)$
8	45	22.5	45	−22.5	$\frac{1}{16}(A+B-2\mathrm{Re}E)$
9	−45	11.25	45	78.75	$\frac{1}{16}(A+B-2\mathrm{Im}E)$

Note: The orientation angle of phase plates (Fig. 2) is measured with respect to a vertical.

then used to normalise the results. Second, as one can see from Table 1, the last four measurements give real or imaginary parts of the complex elements F and D, which correspond to the sines or cosines of the phases in the state (1). Since the phases φ_2, φ_3 are defined on the interval $[0, 2\pi]$, one should know both their cosines and their sines.

The first seven lines of Table 1 describe the measurement of a pure biphoton state. If the state of the biphoton field is mixed, then this set should be completed by two more measurements, providing the real and imaginary parts of the E moment (the eighth and ninth lines in Table 1).

4. Polarisation tomography of single-mode biphotons (experiment)

The method of biphoton tomography described in Section 3 was demonstrated in experiment [24, 25]. The experimental setup is shown in Fig. 3. Pumping was performed by a 120-mW, 351-nm line from a cw argon laser. The pump beam was incident on a lithium iodate ($LiIO_3$) nonlinear crystal of length 1 cm, in which the SPDC radiation was generated. The crystal was cut in such a way that biphotons were emitted in the collinear frequency-degenerate regime. Polarisations of the signal and idler photons were similar, both orthogonal to the pump polarisation (type-I phase matching, also called e−oo interaction). The pump radiation transmitted by the crystal was coupled out from the system by mirror (*2*), which reflected radiation at 351 nm and transmitted radiation at the doubled wavelength. For the spatial and spectral mode selection of SPDC, we used a system of apertures (*4*) and interference filters (*11*), whose transmission spectra had a maximum at the wavelength 700 nm and full width at half maximum 10 nm. The width of the SPDC spectrum for the crystal we used was $\Delta\lambda_{\mathrm{SPDC}} \sim 20$ nm. The angular width of the SPDC correlation function was determined by the pump divergence, $\Delta\theta_{\mathrm{p}} \sim 3 \times 10^{-4}$ rad. The sizes of apertures (*4*) were chosen according to this width. As a result, the finite frequency-angular spectrum of SPDC did not influence polarisation transformation, and the SPDC radiation could be considered as single-mode.

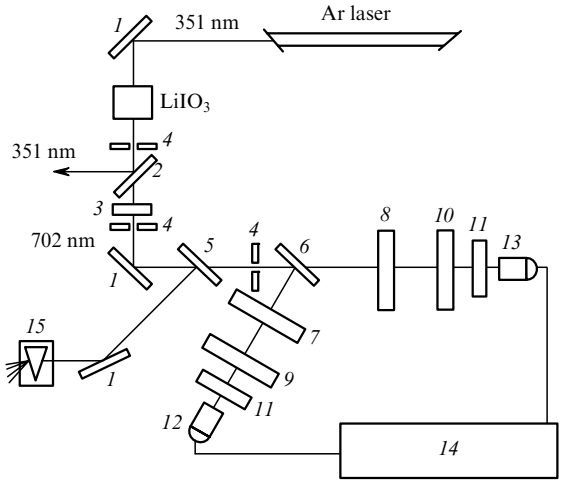

Figure 3. Experimental setup for the quantum tomography of biphoton light: (*1*) mirrors; (*2*) mirror reflecting the UV pump and transmitting the biphoton radiation; (*3*) setting phase plate; (*4*) apertures; (*5*) flipping mirror; (*6*) beamsplitter; (*7*), (*8*) quarter-wave plates; (*9*), (*10*) polarisation prizms; (*11*) interference filters; (*12*), (*13*) photodetectors; (*14*) pair photocount coincidence circuit; (*15*) spectrograph used for observing the spectrum of biphoton light.

Various polarisation states of biphotons were prepared by means of thin quartz plate (*3*) (the setting plate). To find the transformation performed over the polarisation state of the biphoton light, let us write the wavefunction (1) as a column with the elements given by the normalised amplitudes c_i ($i = 1, 2, 3$). The transformation was shown [12] to be described by a 3×3 unitary matrix

$$G \equiv \begin{pmatrix} t^2 & \sqrt{2}tr & r^2 \\ -\sqrt{2}tr^* & |t|^2 - |r|^2 & \sqrt{2}t^*r \\ r^{*2} & -\sqrt{2}t^*r^* & t^{*2} \end{pmatrix}, \qquad (9)$$

so that $|\Psi'\rangle = G|\Psi\rangle$ or

$$\begin{pmatrix} c_1' \\ c_2' \\ c_3' \end{pmatrix} = G \begin{pmatrix} c_1 \\ c_2 \\ c_3 \end{pmatrix}. \qquad (10)$$

The coefficients t and r were introduced in (8). Thus, each set of the two parameters characterising plate (*3*), its thickness and orientation, corresponds to a certain polarisation state (10) at the input of the measurement system.

Since the initial states were prepared by means of an SU(2) transformation, performed by phase plate (*3*), the experiment described here did not result in obtaining a truly arbitrary biphoton–qutrit state. Nevertheless, the qutrit formed behind the plate belonged to a subclass of the state (1), with certain relations between the parameters d_i and φ_i. In experiment, the thickness n of the setting plate was $824 \pm 0.5\,\mu$m and was chosen from the condition that the transformation should not have noticeable frequency dependence within the filter bandwidth. The polarisation state of the biphoton entering the measurement system after transformation in plate (*3*) can be written, according to (10), as

$$\begin{pmatrix} c_1 \\ c_2 \\ c_3 \end{pmatrix} = G \begin{pmatrix} 0 \\ 0 \\ 1 \end{pmatrix}$$

$$= \begin{pmatrix} -0.99 \sin^2 2\alpha \\ 0.998\mathrm{i}\sqrt{2}(-0.0672 - 0.99\mathrm{i}\cos 2\alpha)\sin 2\alpha \\ (-0.0672 - 0.99\mathrm{i}\cos 2\alpha)^2 \end{pmatrix},$$

where the G matrix for the plate with the parameters $\Delta n = n_o - n_e = 0.0089$, $\delta = 32.82$ can be calculated from (9). Here, α is the orientation angle of the plate with respect to the vertical axis, which specifies the state of the qutrit.

The measurement part of the setup consisted of the intensity interferometer (the Brown–Twiss scheme) with nonpolarising 50-% beamsplitter (*6*) and two detectors, (*12*), (*13*) (FEU-79 photomultiplier tubes operating in the photon-counting mode with the quantum efficiency $\eta \sim 10^{-2}$). The beamsplitter was fixed at a small angle ($\sim 12^\circ$) to the beam, in order to keep the polarisation state of light constant after reflection and transmission. Each arm of the interferometer contained quarter-wave phase plate (*7*) or (*8*), and rotatable polarisation filter (*9*) or (*10*) (a Glan–Thompson prism). As quarter-wave plates, we used zero-order quartz plates for the wavelength $\lambda_s = 702$ nm with an AR coating. The losses caused by polarisation filters were of the order of $\sim 8\,\% - 12\,\%$ and the accuracy of their angular alignment was $\sim 2^\circ$. After amplification and amplitude discrimination, the photocounts from the detectors were fed to coincidence circuit (*14*), which had time resolution $T \sim 5$ ns. The frequency-angular spectrum of the biphoton light was studied using ISP-51 spectrograph (*15*).

According to Table 1, a certain set of the fourth-order moments was measured for each orientation of setting plate (*3*). The orientation of polarisation transformers (*7*)–(*10*) in each channel was measured relatively to the polarisation of the initial biphoton beam [prior to the transformation performed by plate (*3*)]. In measurements 1–3, the diagonal elements of the matrix K_4 were determined, while measurements 4–9 provided a combination of diagonal and non-diagonal elements.

The experimental dependences of the amplitudes d_i and phases φ_i for the states prepared with the help of plate (*3*) on the angle of its orientation are presented in Fig. 4. Figure 5 shows the experimental dependences of the elements of the coherence matrix K_4 on α. For comparison, theoretically calculated values of the components d_i and φ_i and the moments D and F are also presented in Figs 4 and 5, respectively. For a fixed orientation of the setting plate, $\alpha_0 = 25^\circ$, the polarisation matrix of the corresponding state was reproduced from the experimental results:

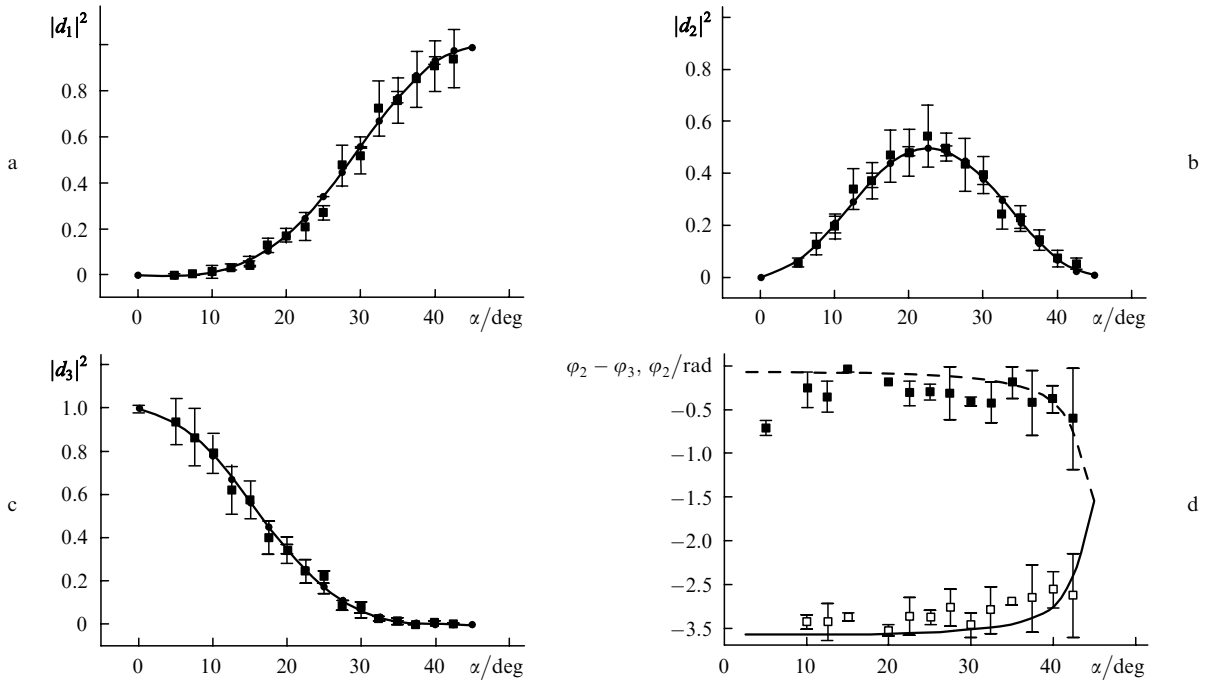

Figure 4. Measurement results for the three amplitudes d_1, d_2, d_3 (■; a, b, c) and two phases φ_2 (■), $\varphi_2 - \varphi_3$ (□) (d). Different initial qutrit states correspond to different orientation angles of setting plate (*3*) (Fig. 2). Solid and dashed curves show the results of calculation.

$$\rho_{\mathrm{ex}} = \qquad (11)$$

$$\begin{pmatrix} 0.271 & 0.345+0.074\mathrm{i} & -0.24-0.114\mathrm{i} \\ 0.345-0.074\mathrm{i} & 0.508 & -0.316-0.075\mathrm{i} \\ -0.24+0.114\mathrm{i} & -0.316+0.075\mathrm{i} & 0.221 \end{pmatrix},$$

The elements of this matrix are in one-to-one correspondence with the measured moments (5). The eigenvalues of the matrix are $\lambda_1 = 0.99$, $\lambda_2 = -0.021$, and $\lambda_3 = 0.03$. The trace of its square is $\mathrm{Tr}\,(\rho_{\mathrm{ex}}^2) = 0.981$.

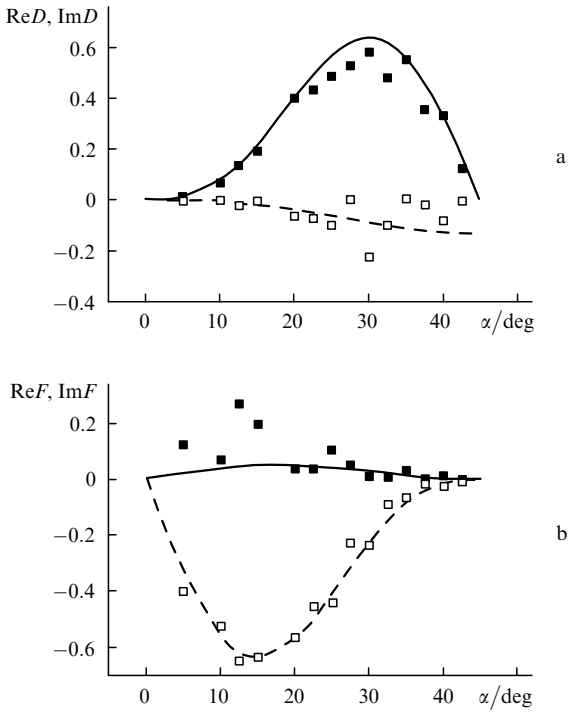

Figure 5. Measured elements of the K_4 matrix. Shown in the plot are the real (■) and imaginary (□) parts of the moments D (a) and F (b). Different initial qutrit states correspond to different orientation angles of setting plate (*3*). Solid and dashed curves show the results of calculation.

One can see from Figs 4, 5 that the largest relative errors appear in the reconstructed phases of the states and the nondiagonal elements of the density matrix. This is because these values are found from the results of several measurements. The errors are summed up and contribute to the final result.

Several remarks about the properties of the restored density matrix ρ_{ex} need to be made. This matrix is Hermitian and normalised, i.e., $\rho_{\mathrm{ex}}^{+} = \rho_{\mathrm{ex}}$; $\mathrm{Tr}\,(\rho_{\mathrm{ex}}) = 1$. It follows from the general properties of density matrices that this matrix should have positive eigenvalues and satisfy the condition $0 < \mathrm{Tr}\,(\rho_{\mathrm{ex}}^2) \leqslant 1$. For pure states, which are discussed here, the matrix should have only a single nondegenerate eigenvalue, equal to unity, and $\mathrm{Tr}\,(\rho_{\mathrm{ex}}^2) = 1$. Because of experimental errors, the restored density matrix ρ_{ex} evidently does not satisfy these requirements. In order to put some 'realistic' physical state, satisfying these properties, in correspondence to the experimentally restored density matrix, a numerical method has been applied. This method, called the root approach to the restoration of qutrits, is comprehensively described in Refs [25, 26].

5. Orthogonality criterion for single-mode biphotons

As we have already mentioned, polarisation tomography of biphoton states implies that in each arm after the beamsplitter (Fig. 2), the unknown input state is projected onto some polarisation state, which is given by the positions of the phase plates and the polarisers. At some positions of these polarisation elements and for a certain input state, the coincidence counting rate in such a system can vanish. It turns out that such a situation is fully equivalent to the orthogonality of the input biphoton state and the pair of single-photon states selected by the polarisation elements in the two channels [27].

Indeed, suppose that in the setup shown in Fig. 2, polarisation states selected in arms 1 and 2 correspond to the modes a_1 and b_2 (the letter denotes a polarisation state and the index numerates the spatial modes), and the state at the input of the setup is [see (2)]

$$|\Psi_{cd}\rangle = \frac{c^{+}d^{+}|\mathrm{vac}\rangle}{|c^{+}d^{+}|\mathrm{vac}\rangle|}. \qquad (12)$$

Here, c^{+}, d^{+} are photon creation operators in the polarisation modes c, d. Note that in the general case, the modes a, b, c, d are not orthogonal. After the beamsplitter, the state vector (12) takes the form

$$|\Psi'_{cd}\rangle = \frac{1}{2|c^{+}d^{+}|\mathrm{vac}\rangle|}$$

$$\times\left(c_1^{+}d_2^{+} + d_1^{+}c_2^{+} + c_1^{+}d_1^{+} + c_2^{+}d_2^{+}\right)|\mathrm{vac}\rangle.$$

The last two terms do not contribute to coincidences because they describe the situation when both photons of the pair are directed to the same detector. Therefore, the coincidence counting rate is given by the second-order intensity correlation function

$$G^{(2)} = \frac{1}{4|c^{+}d^{+}|\mathrm{vac}\rangle|^2}$$

$$\times\langle\mathrm{vac}|(c_1d_2 + d_1c_2)a_1^{+}b_2^{+}a_1b_2(c_1^{+}d_2^{+} + d_1^{+}c_2^{+})|\mathrm{vac}\rangle. \qquad (13)$$

The absence of photocount coincidences for detectors (*8*), (*9*) (Fig. 2) is equivalent to the condition that the correlation function (13) is zero. Since this correlation function is the square of the norm of the state vector $a_1b_2(c_1^{+}d_2^{+} + d_1^{+}c_2^{+})|\mathrm{vac}\rangle$ the condition for the absence of coincidences can be written as

$$a_1b_2(c_1^{+}d_2^{+} + d_1^{+}c_2^{+})|\mathrm{vac}\rangle = 0|\mathrm{vac}\rangle. \qquad (14)$$

Now, the condition for the state selected by the setup to be orthogonal to the state (12) takes the form

$$\langle\Psi_{ab}|\Psi_{cd}\rangle = 0, \qquad (15)$$

where

$$|\Psi_{ab}\rangle = \frac{a^{+}b^{+}|\mathrm{vac}\rangle}{|a^{+}b^{+}|\mathrm{vac}\rangle|}.$$

Condition (15) can be written as

$$\langle \mathrm{vac}|abc^+d^+|\mathrm{vac}\rangle = 0. \quad (16)$$

Note that the state vector $abc^+d^+|\mathrm{vac}\rangle$ contains two creation operators and two annihilation operators; therefore, it is equal to the vacuum state multiplied by some number. Due to (16), this number is zero. Therefore, the orthogonality condition can be written as

$$abc^+d^+|\mathrm{vac}\rangle = 0|\mathrm{vac}\rangle. \quad (17)$$

It is easy to show that the orthogonality condition (17) and the absence of coincidences (14) are equivalent, i.e., the expression on the left-hand side of (17) can be symmetrised with respect to spatial modes. Physically, it follows from the fact that the photons at the input of the Brown–Twiss interferometer differ only in polarisation, so that for a nonpolarising beamsplitter they are indistinguishable.

Thus, the orthogonality condition for two biphotons is equivalent to the absence of coincidences in the scheme shown in Fig. 2 if one of the biphotons is at the input and the setup is 'aligned' to select the second biphoton (filters in the interferometer arms select polarisation states corresponding to the polarisations of the biphoton 'halves'). Note that the states under consideration are quite arbitrary and have an arbitrary polarisation degree, and therefore, the rate of single-photon detector counts is in the general case nonzero. Thus, the described picture corresponds to an anticorrelation effect more general than the well-known 'correlation dip' effect observed earlier for nonpolarised biphotons (biphotons with orthogonal polarisations in pairs) [28].

6. Orthogonality of single-mode biphotons (experiment)

The orthogonality criterion formulated in the previous section was experimentally verified in Refs [29, 30]. The experimental setup is shown in Fig. 6. Pumping was performed by a 13-mW, 325-nm line of a helium–cadmium laser. Type-I SPDC was generated in two BBO crystals of thickness 5 mm. The optic axes of the crystals were orthogonal to each other, so that in the first crystal, the state $|0,2\rangle$ was generated, and in the second one, the state $|2,0\rangle$. A half-wave plate placed into the pump beam before the crystals enabled one to control the ratio of the modules of the corresponding amplitudes. The relative phase ε between the states $|2,0\rangle$ and $|0,2\rangle$ was introduced and varied by tilting two quartz plates of thickness 1 mm, their optic axes being orthogonal to the beam. As a result, after the crystals, the coherent superposition of two states was generated,

$$|\Psi'\rangle = \sin 2\chi|2,0\rangle + \exp(\mathrm{i}\varepsilon)\cos 2\chi|0,2\rangle. \quad (18)$$

Here, χ is the orientation angle for the half-wave plate, measured with respect to the vertical direction. The pump radiation was cut by a mirror, and the biphoton light was directed into a Brown–Twiss interferometer, similar to the one shown in Fig. 2. The frequency selection was performed with an interference filter, with the central wavelength at 650 nm and the bandwidth 10 nm. The angular (spatial) selection was performed by means of a system of apertures. The detection unit consisted of EG&G avalanche diodes operating in photon-counting mode. The signals from the diodes were fed to the coincidence circuit with the time resolution $T = 1.5$ ns.

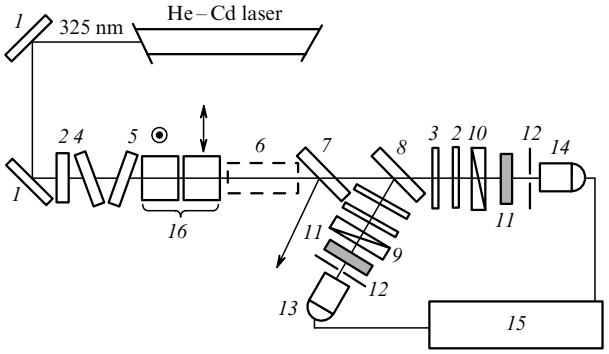

Figure 6. Experimental setup for preparing an arbitrary qutrit state and demonstrating orthogonality of biphotons: (*1*) mirrors; (*2*), (*3*) half- and quarter-wave phase plates; (*4*), (*5*) quartz plates for varying the phase ε; (*6*) the Pockel cell (used only for the preparation of an arbitrary qutrit state, see Section 7); (*7*) mirror reflecting the pump and transmitting biphotons; (*8*) nonpolarising beamsplitter; (*9*), (*10*) Glan–Thompson prisms selecting vertically polarised light; (*11*) interference filters ($\lambda_0 = 650$ nm, $\Delta\lambda = 10$ nm); (*12*) apertures; (*13*), (*14*) photodetectors; (*15*) pair coincidence circuit; (*16*) two crystals of beta-barium borate (BBO), the directions of optic axes are shown above.

Note that the state (18) is specified by only two independent parameters, χ and ε, and hence, it would be impossible to prepare an arbitrary polarisation state of the form (1) in such a scheme. However, the polarisation degree of the state (18) could take any values from 0 to 1.

For testing the orthogonality criterion, as the input state $|\Psi_{cd}\rangle$ we chose a state with the polarisation degree 0.5. It was convenient to pick the state that is depicted on the Poincare sphere as two points placed on the equator at angles $\pm 74.5^\circ$ to the HV axis (Fig. 7). In experiment, the phase ε was set equal to π and the angle χ equal to 15°. There are infinitely many biphotons $|\Psi_{ab}\rangle$ that are orthogonal to $|\Psi_{cd}\rangle$, but if the state of one of the 'halves' of the biphoton $|\Psi_{ab}\rangle$ is fixed, then the state of the other 'half' can be unambiguously determined from the orthogonality condition. In experiment, one of the filters in the Brown–Twiss scheme was aligned for the transmission of light linearly

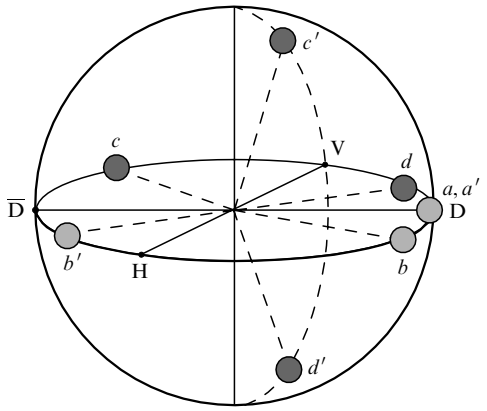

Figure 7. Orthogonal states on the Poincare sphere. Dark circles show the states that are generated in the preparation part. Light circles show states orthogonal to them, which are selected by the Brown–Twiss scheme.

polarised at 45° to the vertical direction. According to the calculation, orthogonality condition is satisfied if the polarisation filter in the other arm transmits light polarised at 60° to the vertical. The corresponding state $|\Psi_{ab}\rangle$ is shown in Fig. 7.

Figure 8 presents the number of photocount coincidences as a function of the angle χ of the half-wave plate orientation, with the polarisation filters in the Brown – Twiss interferometer selecting the state $|45^\circ, 60^\circ\rangle$. One can see that the minimum of the coincidence counting rate corresponds to $\chi = 15^\circ$, in agreement with the calculation. Then, the plate was fixed in this position, and the number of coincidences was measured versus the polariser orientation in the second arm of the Brown – Twiss setup. The filter in the first arm still selected linear polarisation at 45° to the vertical. According to the calculation, the minimum of coincidence counting rate corresponded to the angle 60° (Fig. 9).

Further rotation of the half-wave plate turned the state into $|0, 2\rangle$ (at $\chi = 45^\circ$) and then, because of a stepwise change in the pump phase by π, the two points depicting 'halves' of the biphoton started traveling along the meridian of the Poincare sphere (Fig. 7). At $\chi = 75^\circ$, polarisation degree was again 0.5, but this time, the state $|\Psi_{cd}\rangle$ consisted of two elliptically polarised photons. One can easily see that in this case, the orthogonality condition was satisfied when the Brown – Twiss scheme selected the state $|45^\circ, -60^\circ\rangle$. As one can see from Fig. 10, for this configuration the minimum of the coincidence counting rate also occurred at the theoretically calculated angle $\chi = 75^\circ$.

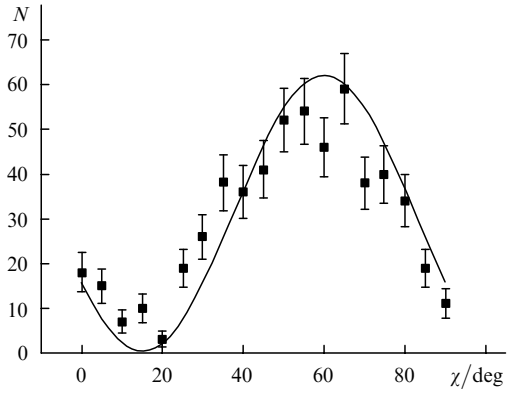

Figure 8. Dependence of the coincidence number N in 40 s on the rotation angle χ of the half-wave plate in the pump beam. The analysers are aligned for transmitting light linearly polarised at angles 45° and 60° to the vertical direction. The minimum of the coincidence counting rate corresponds to the generation of the state orthogonal to the one selected by the scheme.

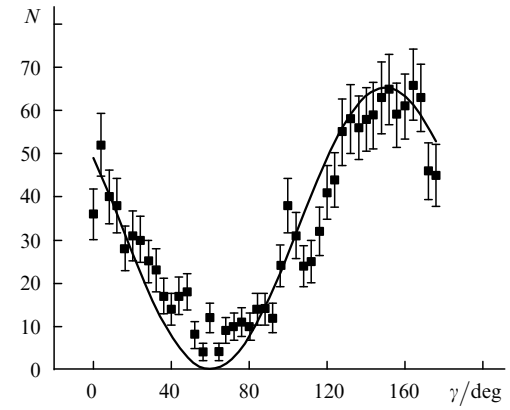

Figure 9. Coincidence number N in 100 s versus the rotation angle χ of the analyser in one of the arms of the Brown – Twiss scheme. The second analyser is aligned for transmitting light polarised linearly at an angle 45° to the vertical direction. The orientation angle of the half-wave plate in the pump beam is $\chi = 15^\circ$.

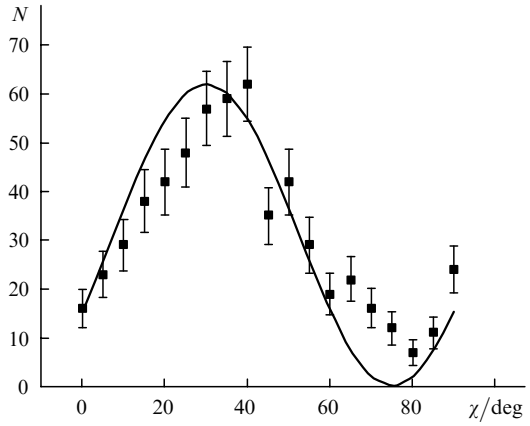

Figure 10. Coincidence number N in 100 s as a function of the rotation angle χ of the half-wave plate in the pump beam. In this case, the biphoton is formed by two elliptically polarised photons. The analysers are aligned for transmitting light linearly polarised at angles 45° and −60° to the vertical direction.

The coincidence counting rate was also measured as a function of the phase ε. In this case, the half-wave plate was fixed at the angle $\chi = 15^\circ$ and the filters selected the state $|45^\circ, 60^\circ\rangle$. According to the calculation, the minimum of coincidences was observed at $\varepsilon = \pi$.

7. Preparation of an arbitrary biphoton state

In the previous section, we discussed an experimental scheme that allowed one to generate states with an arbitrary polarisation degree. However, in practice it is often necessary to prepare a qutrit in an arbitrary state. This requires a possibility to independently vary four parameters determining the state (1). This is possible by using an interferometric setup for preparing qutrit states [31] but this setup has a serious drawback, which is an obstacle for using it in practice, – its time instability. It turns out that this drawback can be avoided. One can do without an interferometer by slightly improving the scheme shown in Fig. 6. In order to generate an arbitrary state, one should add two more controllable parameters to χ and ε [the two parameters characterising the state (18)]. As these parameters, one can take the optical thickness $\xi = L\Delta n/\lambda$ (with L being the plate thickness and Δn the birefringence) and the orientation β of a phase plate introduced into the biphoton beam in the state (18). Passing from the state (18) to the state (1) with the help of an arbitrary phase plate can be demonstrated by means of a simple geometric transformation on the Poincare sphere (see [30]).

In order to vary the optical thickness ξ arbitrarily from 0 to 2π, a Pockel cell can be used, as it was done in Ref. [30]. The parameter β (orientation) was varied continuously by

rotating the cell in the biphoton beam. The Pockel cell was made of a lithium niobate crystal of length 3 cm, its optic axis Z coinciding with the direction of the biphoton beam. With a DC voltage applied along the X crystallographic axis, due to the electrooptic effect the crystal became biaxial. The plane containing the optic axes was oriented at 45° to the XZ plane. The phase delay between the 'extraordinary' wave (polarised linearly in the plane of the optic axes) and the 'ordinary' wave (polarised linearly at $-45°$ to the plane XZ) was varied from 0 to 2π as the DC voltage varied from 0 to 2.8 kV. In this case, the Pockel cell was similar to a zero-order phase plate (since the induced birefringence was small) with ξ varying from 0 to 2π.

At the beginning, the half-wave plate in the pump beam was fixed at the angle $\chi = 22.5°$ and the phase ε was fixed at π. The initial orientation of the cell corresponded to the vertical direction of the optic axis. The initial voltage applied to the Pockel cell was zero. As a result, the state (18) was initially transformed into the state $|\mathrm{D}, \overline{\mathrm{D}}\rangle$ and caused a maximum of the coincidence counting rate in the Brown–Twiss scheme, where the polarisation filters selected the states $+45°$ (in the upper arm) and $-45°$ (in the lower arm). Further, the orientation of the Pockel cell was kept the same but a halfwave voltage was applied to it. The state of the biphoton light remained the same, since the transformation performed by the Pockel cell was the rotation of the state on the Poincare sphere by π around the HV axis. Keeping the Brown–Twiss scheme aligned for selecting the state $|\mathrm{D}, \overline{\mathrm{D}}\rangle$ and rotating the Pockel cell with $\xi = \pi/2$, one could expect the coincidence counting rate to turn to zero at $\beta = 22.5°$, since in that case the state $|\mathrm{D}, \overline{\mathrm{D}}\rangle$ was transformed into the orthogonal state $|\mathrm{H}, \mathrm{V}\rangle$ (Fig. 7). Figure 11 shows the dependence of the coincidence counting rate on the angle β; indeed, the minimum of the dependence occurs at $\beta = 22.5°$. Further, if the orientation of the Pockel cell is fixed at $\beta = 22.5°$ and the DC voltage applied to the cell is varied from 0 to 2.8 kV, one should expect a minimum of coincidence counting rate if the applied voltage corresponds to the half-wave value. The corresponding dependence of the coincidence counting rate on ξ is shown in Fig.12. At $\xi = \pi/2$, a minimum of the coincidence counting rate was

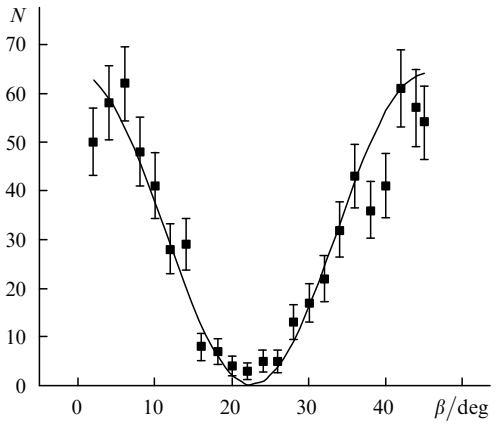

Figure 11. Coincidence number N in 80 s versus the rotation angle β of the Pockel cell. The analysers are aligned for transmitting light linearly polarised at angles 45° and $-45°$ to the vertical direction. The minimum corresponds to the generation of the state $|\mathrm{H}, \mathrm{V}\rangle$ orthogonal to the state $|\mathrm{D}, \overline{\mathrm{D}}\rangle$. The voltage applied to the Pockel cell corresponds to the optical phase thickness $\xi = \pi/2$.

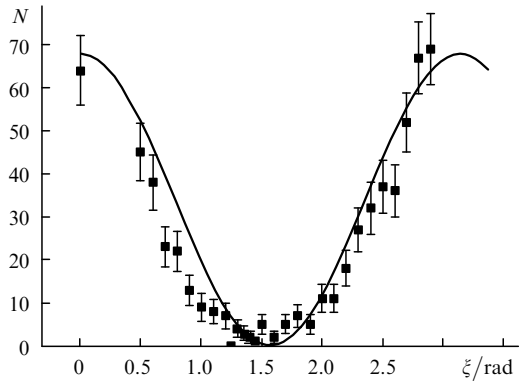

Figure 12. Dependence of the coincidence number N in 80 s on the optical phase thickness ξ of the Pockel cell (ξ varied from 0 to π as the voltage applied to the Pockel cell varied from 0 to 2.8 kV). The Pockel cell orientation angle β is fixed at $\beta = 22.5°$. Similarly to the previous case, the minimum of coincidences corresponds to the generation of the state $|\mathrm{H}, \mathrm{V}\rangle$, which is orthogonal to $|\mathrm{D}, \overline{\mathrm{D}}\rangle$.

observed. As in the previous case, the minimum was due to the orthogonality of the states $|\mathrm{H}, \mathrm{V}\rangle$ and $|\mathrm{D}, \overline{\mathrm{D}}\rangle$.

8. 'Ternary logic'

As we have shown in Section 2, polarised biphotons are qutrits, i.e., quantum objects with three basic states. By choosing an orthogonal basis in the space of polarised biphotons and preparing the basic states $|\Psi_0\rangle$, $|\Psi_1\rangle$, $|\Psi_2\rangle$, one can encode quantum information in qutrits and pass in this way from binary quantum information protocols to ternary ones.

There are infinitely many ways to prepare the three basic states. The easiest way is to prepare the states $|2, 0\rangle$, $|1, 1\rangle$, $|0, 2\rangle$, which are 'naturally' generated in experiment. However, in some cases it is more convenient to work with the states that have the same degree of polarisation and hence can be easily transformed into each other by linear polarisation transformations. In Ref. [32], three mutually orthogonal biphoton states with zero degree of polarisation (consisting of orthogonally polarised photons) were prepared in experiment. These were the following three states: a pair of photons polarised horizontally and vertically, $|\mathrm{H}, \mathrm{V}\rangle$, a pair of photons polarised linearly at angles $\pm 45°$ to the vertical, $|\mathrm{D}, \overline{\mathrm{D}}\rangle$, and a pair of photons with right and left circular polarisations, $|\mathrm{R}, \mathrm{L}\rangle$.

The states $|\mathrm{H}, \mathrm{V}\rangle$, $|\mathrm{D}, \overline{\mathrm{D}}\rangle$ and $|\mathrm{R}, \mathrm{L}\rangle$ can be easily transformed into each other by means of phase plates. Indeed, it was shown in Ref. [32] that a half-wave plate oriented at the angle 22.5° to the H axis transforms $|\mathrm{D}, \overline{\mathrm{D}}\rangle$ into $|\mathrm{H}, \mathrm{V}\rangle$ and a quarter-wave plate oriented at the angle 45° to the H axis transforms $|\mathrm{R}, \mathrm{L}\rangle$ into $|\mathrm{H}, \mathrm{V}\rangle$. The transformation from $|\mathrm{R}, \mathrm{L}\rangle$ to $|\mathrm{D}, \overline{\mathrm{D}}\rangle$ can be performed by means of a quarter-wave plate oriented along the H axis.

A similar orthogonal basis can be constructed of states that can be transformed into each other by using a single phase plate. This was done in Ref. [33]; the states were also composed of orthogonally polarised photons (and could be shown as opposite points on the Poincare sphere in Fig. 1).

Polarisation states of two-photon light and their transformations can be employed for the transmission of quantum information in ternary encoding. As the basic

states, one can use not only the states $|H, V\rangle$, $|D, \overline{D}\rangle$ and $|R, L\rangle$, but any three orthogonal states. Distinguishing between the three orthogonal qutrits may be performed by means of the orthogonality criterion: if the setup is 'aligned' to select some qutrit, no coincidence can occur if the qutrit at the input is orthogonal to it. A coincidence means that the qutrit at the input coincides with the one selected by the setup. (Even in this case, the probability of a coincidence is less than 100 %.) Qutrit encoding of quantum information was first performed in Ref. [5] but only for the case of noncollinear (two-beam) SPDC. Encoding was based on the three states of the Bell basis; one of the Bell states (the singlet state $|\Psi^-\rangle$) was not used.

Ternary encoding of quantum information is actively discussed in the literature. For instance, a ternary protocol for quantum cryptography was suggested [34], which is a qutrit counterpart of the well-known BB84 protocol [35] for qubits. Theoretically, ternary quantum information protocols have some advantages over the corresponding binary protocols. Ternary coding enables one to increase the data transmission rate [36] and safety against eavesdropping attacks [37]. In the ternary quantum cryptography protocol proposed in Ref. [34], the expressions for the qutrit states participating in the data transmission were obtained. In contrast to the binary BB84, which employs four states constituting two mutually unbiased bases, the ternary protocol uses twelve states forming four bases. The authors of Ref. [34] did not specify the physical origin of the qutrits participating in the protocol; expressions for the twelve states were given in the general form, in terms of some initial states.

In Ref. [38], the corresponding twelve states were considered for the case of biphoton qutrits. The states were calculated and shown on the Poincare sphere. An experimental setup was proposed that could be used for the realisation of the protocol suggested in Ref. [34].

9. Conclusions

In this review, we tried to summarise a series of experimental and theoretical papers devoted to the polarisation properties of biphoton fields and carried out in the Chair of Quantum Electronics at the Department of Physics of MSU during the recent years. These works are much related to the interference of biphoton fields but are more focused on the application of such fields in quantum information. In all these works, a biphoton is treated as a qutrit, a ternary unit of quantum information. Biphoton qutrits have been studied from the viewpoint of their symmetry and transformations, a technique for their preparation has been suggested and realised in experiment, the measurement procedure has been developed, and a method for distinguishing between orthogonal states has been proposed. Finally, a biphoton-based ternary protocol of quantum cryptography has been suggested. Summarising, one can say that the elemental base for practical implementation of biphotons in quantum information has been developed.

Will this direction of research be prominent in practice? The answer depends on the possibility to simplify the generation of biphoton light. At present, generation of biphotons is mastered in scientific laboratories but this is not sufficient for practical applications. The generation of two-photon light requires using high-power pump lasers. It is possible that requirements to the pump radiation can be substantially alleviated if the two-photon light is obtained, instead of SPDC, via hyper-parametric down-conversion (four-wave mixing in the spontaneous regime, when there is only one pump beam at the input, and two photons of the pump give rise to a biphoton). This effect can be observed in optical fibers; in this case, due to a large interaction length and the quadratic dependence of the effect of the pump intensity, rather 'bright' biphoton light can be generated from a weak diode laser. This method of producing biphoton fields is already developed in some laboratories (see, for instance, [39]).

Acknowledgements. This work was supported in part by the Russian Foundation for Basic Research (Grant Nos 02-02-16664 and 03-02-16444), INTAS 2122-01, the program 'The Support of Scientific Schools' (Project No. 166.2003.02) and the Special Federal Program 'Research and Developments in the Priority Fields of Science and Technology Development' (item 15 of section 'Basic Research in the Field of Physics' of the block 'Specialized Basic Rresearch'). One of the authors (L.K.) is grateful to the support of INTAS (Grant No. 03-55-1971).

References

1. Bennett C.H. *Physics Today*, October, 24 (1995).
2. Kilin S.Ya. *Usp. Fiz. Nauk*, **169**, 507 (1999).
3. Braunstein S.L., Mann A., Revzen M. *Phys. Rev. Lett.*, **68**, 3259 (1992).
4. Braunstein S.L., Mann A. *Phys. Rev. A*, **51**, R1727 (1995).
5. Mattle K., Weinfurter H., Kwiat P.G., Zeilinger A. *Phys. Rev. Lett.*, **76**, 4656 (1996).
6. Brida G., Genovese M., Novero C. *J. Mod. Opt.*, **47**, 2099 (2000).
7. Pan J.-W., Bouwmeester D., Weinfurter H., Zeilinger A. *Phys. Rev. Lett.*, **80**, 3891 (1998).
8. Bouwmeester D., Pan J.-W., Mattle K., Eibl M., Weinfurter H., Zeilinger A. *Nature*, **390**, 575 (1998); Boschi D., Branca S., De Martini F., Hardy L., Popescu S. *Phys. Rev. Lett.*, **80**, 1121 (1998); Furasawa A., Sorensen J.L., Braunstein S.L., Fuchs C.A., Kimble H.J., Polzik E.S. *Science*, **282**, 706 (1998); Kim Y., Kulik S.P., Shih Y. *Phys. Rev. Lett.*, **86**, 1370 (2001).
9. Ekert A.K. *Phys. Rev. Lett.*, **67**, 661 (1991); Ekert A.K., Rarity J.G., Tapster P.R., Palma G.M. *Phys. Rev. Lett.*, **69**, 1293 (1992).
10. James D.F.V., Kwiat P.G., Munro W.J., White A.G. *Phys. Rev. A*, **64**, 052312 (2001).
11. Klyshko D.N. *Zh. Eksp. Teor. Fiz.*, **111** (6), 1955 (1997).
12. Burlakov A.V., Klyshko D.N. *Pis'ma Zh. Eksp. Teor. Fiz.*, **69**, 795 (1999).
13. Thew R.T., Nemoto K., White A.G., Munro W.J. *Phys. Rev. A*, **66**, 012303 (2002).
14. Bouwmeester D., Ekert A., Zeilinger A. *The Physics of Quantum Information* (Heidelberg, New York: Springer-Verlag 2000; Moscow: Postmarket, 2002).
15. Shercliff W.A. *Polirized Light. Production and Use* (Cambridge, Massachusetts: Harvard University Press, 1962; Moscow: Mir, 1965).
16. Burlakov A.V., Chekhova M.V. *Pis'ma Zh. Eksp. Teor. Fiz.*, **75** (8), 505 (2002).
17. Alodzhants A.P., Arakelyan S.M., Chirkin A.S. *Zh. Eksp. Teor. Fiz.*, **108**, 63 (1995).
18. Usachev P., Soderholm J., Bjork G., Trifonov A. *Opt. Commun.*, **193**, 161 (2001).
19. Korolkova N., Leuchs G., Loudon R., Ralph T., Silberhorn C. *Phys. Rev. A*, **65**, 052306 (2002).
20. Smithey D.T., Beck M., Raymer M.G., Faridani A. *Phys. Rev. Lett.*, **70**, 1244 (1993).

21. D'Ariano G.M., Macchiavello C., Paris M.G.A. *Phys. Rev. A*, **50**, 4298 (1994).
22. Leonhardt U., Paul H., D'Ariano G.M. *Phys. Rev. A*, **52**, 4899 (1995).
23. Bushev P.A., Karasev V.P., Masalov A.V., Putilin A.A. *Opt. Spektrosk.*, **91**, 558 (2001).
24. Krivitskii L.A., Kulik S.P., Penin A.N., Chekhova M.V. *Zh. Eksp. Teor. Fiz.*, **124** (4), 1 (2003).
25. Bogdanov Yu.I., Chekhova M.V., Krivitsky L.A., et al. *Phys. Rev. A*, **70**, 04230 (2004).
26. Bogdanov Yu.I., Krivitskii L.A., Kulik S.P. *Pis'ma Zh. Eksp. Teor. Fiz.*, **78** (6), 804 (2003).
27. Zhukov A.A., Maslennikov G.A., Chekhova M.V. *Pis'ma Zh. Eksp. Teor. Fiz.*, **76**, 696 (2002).
28. Hong P.C.K., Ou Z.Y., Mandel L. *Phys. Rev. Lett.*, **59**, 2044 (1987); Shih Y.H., Alley C.O. *Phys. Rev. Lett.*, **61**, 2921 (1988).
29. Chekhova M.V., Krivitsky L.A., Kulik S.P., Maslennikov G.A. *Phys. Rev. A*, **70**, 032332 (2004).
30. Krivitskii L.A., Kulik S.P., Maslennikov G.A., Chekhova M.V. *Zh. Eksp. Teor. Fiz.*, **127** (3), 1 (2005).
31. Bogdanov Yu., Chekhova M., Kulik S., Maslennikov G., Zhukov A., Oh C.H., Tey M.K. *Phys. Rev. Lett.*, **93**, 230503 (2004).
32. Burlakov A.V., Chekhova M., Karabutova O.A., Klyshko D.N., Kulik S.P. *Phys. Rev. A*, **60**, R4209 (1999).
33. Tsegaye B.T., Soderholm J., Atature M., Trifonov A., Bjork G., Sergienko A.V., Saleh B.E.A., Teich M.V. *Phys. Rev. Lett.*, **85**, 5013 (2000).
34. Bechmann-Pasquinucci H., Peres A. *Phys. Rev. Lett.*, **85**, 3313 (2000).
35. Bennett C.H., Brassard G. *Proc. IEEE Int. Conf. on Computers, Systems and Signal Processing* (Bangalore, India; New York: IEEE, 1984) p. 175.
36. Bechmann-Pasquinucci H., Tittel W. *Phys. Rev. A*, **61**, 062308 (2000).
37. Bruss D., Machiavello C. *Phys. Rev. Lett.*, **88**, 127901 (2002).
38. Chekhova M.V., Maslennikov G.A., Kulik S.P., Zhukov A.A. *J. Opt. B*, **5**, 530 (2003).
39. Fiorentino M., Voss P.L., Sharping J.E., Kumar P. *IEEE Photon. Techn. Lett.*, **14** (7), 983 (2002).